On the stability of aqueous dispersions containing conducting colloidal particles.

Szparaga, Ryan; Woodward, Clifford E; Forsman, Jan

Published in:
Soft Matter

DOI:
10.1039/c5sm00161g

2015

On the stability of aqueous dispersions containing conducting colloidal particles

Ryan Szparaga*, Clifford E. Woodward** and Jan Forsman*
Theoretical Chemistry, Lund University
P.O.Box 124, S-221 00 Lund, Sweden
*School of Physical, Environmental and Mathematical Sciences
University College, University of New South Wales, ADFA
Canberra ACT 2600, Australia

March 15, 2015

Abstract

We use a combination of simulations and a simple theoretical approach to investigate interactions between neutral conducting surfaces, immersed in an electrolyte solution. The study is conducted at the primitive model level, which necessitates the use of multiple image reflections. Our approximate theory is based on a classical density functional formulation of Poisson-Boltzmann theory. The same approach can in principle also be imported to more advanced treatments, where ion correlations are accounted for. An important limiting result that guides our treatment of the image forces, is that the repulsive salt-induced interactions cancel the attractive zero frequency van der Waals attraction at long range. That is, at vanishing frequency, the van der Waals interaction between the conducting surfaces is, at large separations, perfectly screened by the intervening salt solution. The simulations are computationally intensive, due to a strong dependence upon the number of image reflections used, with especially poor convergence when an odd number of images is used. We demonstrate that our approximate density functional approach is remarkably accurate, even in the presence of a 2:1 salt, or when the surfaces preferentially adsorb one ion species. The former observation was rather unexpected, given the lack of ion correlations within our mean-field treatment, and is most likely due to a cancellation between two opposing effect, both of which are generated by ion correlations.

1 Introduction

Dispersions containing conducting particles are not only theoretically interesting, but find many practical applications. The various versions of colloidal gold, first produced by Faraday,[1] are well-known though the most commonly used method of synthesis was developed by Turkevich.[2] In recent years, gold nanoparticles have found a wide range of applications, including non-linear optics, biology and catalysis.[3] The mechanisms leading to the stability of colloidal gold sols are still being debated, with some conflict between experimental results and theoretical conjectures. Sometimes stabilizers are added to prevent flocculation in these systems, but it is also possible to produce stabilizer-free gold sols with a long shelf-life.[4–8] It has even been suggested that large particles can be re-dispersed, in a process called "digestive ripening".[7] The stability of the sols will depend upon pH and ionic strength and it is generally believed that the adsorption of citrate ions (which are utilized as a reducing

agents in the Turkevich method) onto the gold particles, renders them negatively charged. This surface charge subsequently creates a free energy barrier to flocculation. Although this barrier can be substantial, most dispersions containing charged colloidal particles are not at a free energy minimum, being thermodynamically metastable. It is also possible to create metastable dispersions in the absence of citrate ions, provided that the solution does contain other anions that displays a preferential adsorption at a gold surface.[9] Similar approaches can be used to stabilize colloidal silver.[10]

A simple (and by far the most commonly used) theoretical description of interparticle interactions in these systems, is afforded by the DLVO theory.[11,12] Here, the total interaction between particles is composed of two additive terms, one stemming from attractive van der Waals (vdW) interactions, while the other originates from salt-screened Coulombic repulsions between charged particles. If the colloidal particles are *not* charged, DLVO theory predicts attractive interactions between particles. The effect of dielectric inhomogeneities, e.g., that at the interface between the electrolyte solution and the particle surfaces, are generally neglected in DLVO theory. The interface physically manifests itself as varying solvation conditions for the ions in the electrolyte. When ions are close to the particle surfaces their solvation shells become compromised, which may cause the free energy to either increase or decrease, depending upon the nature of the solvent and the surface. In a continuum model, this can be described in terms of image charge interactions. For conductive particles, this can give rise to a stabilizing effect on the particle dispersion, though this mechanism is not generally considered in these systems.[4,13,14]

This work will hopefully pave the way for future studies on the stability of metal particle dispersion, with more focused modelling of specific systems, such as gold sols. The scope of the present work is limited to a general treatment of relevant electrostatic mechanisms in such systems. One important limitation of our work is that we will only consider zero frequency contributions. Our specific aims are:

- To generate simulation data for ion-induced interactions between perfectly conducting surfaces. Such simulations have (to the best of our knowledge) never been conducted before, and since simulated data are essentially exact, for a given model system (within statistical noise), they will serve as an important reference with which we can evaluate more approximate approaches.
- To construct an approximate theoretical treatment that is based on an ion-surface Hamiltonian, i.e. that can be used to evaluate effects from non-electrostatic ion-surface interactions in a realistic manner. Since metal particles often are stabilized (or believed to be stabilized) by adsorbed multivalent ions, we furthermore aim for a theory that is reasonably accurate also for more challenging systems, in which the salt solution contains asymmetric salts (2:1 etc.).

Interactions between surfaces that are dielectrically disparate from the salt solution into which they are immersed, have been studied quite extensively in the past using analytical and semi-analytical approaches.[15–23] We aim to complement these theoretical studies with simulation methods as well as a novel approximate approach. We will simplify the model system by treating spherical colloidal particles as two flat (perfectly conducting) surfaces, implicitly assuming the validity of the Derjaguin approximation.[24] We will also assume that the electrolyte is an aqueous solution, although this restriction can in principle be lifted. The so-called Primitive Model is used, wherein the solvent is treated as a continuum with a bulk dielectric constant, determined *a priori* . Surprisingly, there appears to have been no similar simulation studies of interacting conducting surfaces in salt solutions previously, even at the Primitive Model level. However, we have found that these simulations turn out to be computationally intensive, which might be part of the reason why they have not been performed before.

There is a somewhat deeper connection between solving the electrostatic problem in the presence of images and the role of the zero frequency van der Waals contribution to the

surface-surface interaction.[15,20,25] The dielectric boundaries influence the thermal fluctuations in the degrees of freedom of the surface and solvent media. This gives rise to the zero frequency van der Waals interaction, which is screened in the presence of the electrolyte. The electrostatic potential in the presence of the dielectrics (obtained via the use of images), neglects the fluctuations in the polarizable media. Thus, once the electrostatic free energy is obtained, the zero frequency van der Waals interaction must be added to give the correct total surface potential of mean force. We note that in our study we do not include finite frequency contributions to dispersion interactions, which may prove to be important for specific systems.

In addition to simulations, we will describe an approximate theoretical approach, based on a phenomenological generalization of the Poisson-Boltzmann theory to include the effect of images. We shall call this the image Poisson-Boltzmann (iPB) theory. By making direct comparisons with simulation data, we will show that the iPB theory is remarkably accurate, even for systems containing asymmetric salts. The iPB theory appears to provide a more complete (yet still simple) description of dispersions of conducting particles than is afforded by the DLVO approach.

2 Models and Theory

2.1 Simulation model

The ions in the electrolyte are modelled as monovalent hard spheres, with a common hard sphere radius, R, of 1.5 Å. Using the standard primitive model, water only enters implicitly, via its dielectric constant, $\epsilon_r = 78.3$. The temperature is set to 298 K, which results in a Bjerrum length $l_B = \frac{e^2}{4\pi\epsilon_0\epsilon_r kT} \approx 7.16$ Å, where k is Boltzmann's constant, while ϵ_0 is the dielectric permittivity of vacuum. The electrolyte, filling the gap between two conducting surfaces is in chemical equilibrium with a bulk salt solution, at some specified chemical potential. This system is treated with the usual Grand Canonical Metropolis Monte Carlo schemes. Electrostatic ion-surface interactions (polarization) are handled by image charges, and a hard wall repulsion prevents the ions from approaching the plane of dielectric discontinuity. That is, as the two parallel surfaces are located at $z = 0$ and h, the semi-infinite region of ion confinement is given by $R \leq z \leq (h - R)$. In order to model softly repulsive surfaces, as well as effects from ion-specific adsorption, we will also include a non-electrostatic short-ranged surface potential $w(z)$, which is defined (at the left wall) as:

$$\beta w_{\pm} = \begin{cases} 0, & z > z_c^{\alpha} \\ A_{\pm}(\frac{z}{z_c} - 1)^2, & 0 \leq z \leq z_c^{\alpha} \\ \infty, & z \leq 0 \end{cases} \tag{1}$$

where $A_{\pm}$ is an amplitude factor for cations and anions, respectively (with obvious notation), while β is the inverse thermal energy. The special case $A_+ = A_- = 0$ signifies hard, conducting surfaces. The range of the surface potential is defined by $z_c = 4.5$ Å. The complete non-electrostatic surface interaction, $W(z, h)$, is is symmetric, i.e. $W_{\pm}(z, h) = w_{\pm}(z) + w_{\pm}(h - z)$.

The total interaction energy, βU, for a specific ion configuration $\{\mathbf{r}_i\} \equiv \{x_i, y_i, z_i\}$, can thus be written as:

$$\beta U = \frac{l_b}{2} \sum_i \sum_{j \neq i} \frac{\xi_i \xi_j}{[\rho_{ij}^2 + (z_i - z_j)^2]^{1/2}} + \sum_i W_i(z_i, h) + \beta U_{im}(\{\mathbf{r}_i\}) \tag{2}$$

where $\rho_{ij}^2 = (x_i - x_j)^2 + (y_i - y_j)^2$, ξ_i is the valency ($+1$ or -1) of ion i, while $\beta U_{im}(\{\mathbf{r}_i\})$ is the total image charge interaction energy, resulting from multiple reflections across the left

and right surfaces:

$$\beta U_{im} \approx -\frac{l_b}{2}\sum_{k=1,3\ldots}^{k_{max}}\sum_i\sum_j \xi_i\xi_j\left[\frac{1}{[\rho_{ij}^2+((k-1)h+z_i+z_j)^2]^{1/2}}+\frac{1}{[\rho_{ij}^2+((k+1)h-z_j-z_i)^2]^{1/2}}\right]+$$
$$\frac{l_b}{2}\sum_{m=2,4\ldots}^{m_{max}}\sum_i\sum_j \xi_i\xi_j\left[\frac{1}{[\rho_{ij}^2+(mh+z_i-z_j)^2]^{1/2}}+\frac{1}{[\rho_{ij}^2+(mh+z_j-z_i)^2]^{1/2}}\right] \quad (3)$$

where we have explicitly noted that the infinite sum has to be truncated in practice. It is useful to define the total number of reflections, n_{max}, as $n_{max} = max(k_{max}, m_{max})$. A remarkable finding in this work was the extremely poor convergence that results if an odd number of total reflections (odd n_{max}) is used. This is described in more detail in the Supporting Information, SI. The component of the internal slit pressure tensor that acts normal to the surfaces was evaluated across the mid plane of the slit, as well as at the walls. Agreement between these was used as a convergence check, except at low salt concentrations, in which case the wall evaluations were too noisy to be useful.

Periodic boundary conditions were applied in the directions (x, y) parallel with the surfaces, using the minimum image convention to truncate ion-ion interactions. A long-range correction, to the interactions within the slit region, was applied,[26] but in reality our systems were large enough for this to be insignificant.

2.2 Zero frequency van der Waals attraction (vdW(0))

In this work, we focus on general effects due to differences in static dielectric properties, i.e. we will ignore higher frequency dispersion contributions, although the influence of those will be discussed in the summarizing section. The zero frequency van der Waals (vdW) pressure, $P_{vdW}(0)$, can be written as:[15,25]

$$\beta P_{vdW}(0) = -\frac{\zeta(3)}{8\pi h^3} \quad (4)$$

where $\zeta(n)$ is the Riemann zeta function. This expression is specific to the case where a dielectric medium, separates two semi-infinite conducting slabs. The corresponding vdW interaction free energy is:

$$\beta g_{vdW}(0) = -\zeta(3)/(16\pi h^2) \quad (5)$$

As noted in the Introduction, the effect of intervening salt is to screen $P_{vdW}(0)$ so that it no longer has an algebraic decay.[25] The ionic contribution to the surface pressure (in the presence of the dielectric discontinuities), does not include $P_{vdW}(0)$, as the dielectric media respond passively to the ions (i.e., dielectric fluctuations are ignored in the Primitive Model). Thus the electrostatic surface pressure must contain a long-ranged term, which is equal to -$P_{vdW}(0)$, and thus cancels the zero frequency vdW interaction when it is added.[15,25]

2.3 "Image Poisson-Boltzmann" theory (iPB)

The simulations, described above, are computationally expensive due to the large system sizes, many image reflections, and the need for a large number of simulated configurations in order to achieve satisfactory precision and accuracy (see below). Hence, we have also developed an approximate, but computationally inexpensive, description for these systems, which extends the well-known Poisson-Boltzmann (PB) theory. We use the classical density functional formulation of this theory,[27,28] wherein the free energy functional, $\mathcal{F}[n_\alpha(\mathbf{r})]$, can be written as:

$$\beta\mathcal{F}[n_\xi(\mathbf{r})] = \int\sum_{\xi=+,-} n_\xi(\ln[n_\xi(\mathbf{r})]-1)d\mathbf{r} +$$

$$\frac{l_B}{2}\int\int\sum_{\xi=+,-}\sum_{\xi'=+,-} n_\xi(\mathbf{r})n_{\xi'}(\mathbf{r}')\frac{\xi\xi'}{|\mathbf{r}-\mathbf{r}'|}d\mathbf{r}d\mathbf{r}' + \beta\int\sum_{\xi=+,-}(W_\xi(\mathbf{r})+V_{im}(\mathbf{r}))n_\xi(\mathbf{r})d\mathbf{r}, \quad (6)$$

Here, n_ξ is the density of ions with valency ξ, while V_{im} is a potential due to image interactions. The slit geometry, in combination with the mean-field characteristics of the PB theory, allows us to integrate along the (x, y) directions parallel with the surfaces, leaving only z dependent quantities. The interaction free energy per unit area, g_s, can be obtained as:

$$g_s = \mathcal{F} - \sum_{\xi=+,-}\left(\mu_\xi\int_0^h n_\xi(z)dz + kTn_\xi^b\right) \quad (7)$$

where μ and n^b denotes chemical potential and bulk density, respectively. It is convenient to measure interaction free energies relative to the bulk, or to the value at some large separation. More specifically, we use the following approximate expression $\Delta g_s \equiv g_s(h) - g_s(h_{max})$, with $h_{max} - 2R = 400$ Å. We define the corresponding zero frequency vdW quantity (vdW(0)) in an analogous fashion: $\Delta g_{vdW}(0;h) \equiv g_{vdW}(0;h) - g_{vdW}(0;h_{max})$. The net pressure is given by $\Delta P \equiv P(h) - P_b$, where $P(h)$ is the salt-induced internal slit pressure, while P_b is the bulk pressure.

The image potential, V_{im} represents the effect of the dielectric discontinuity on the ionic free energy. In the usual PB theory, this term is zero, which is due to the fact that the PB theory is a mean-field approximation. The reason why V_{im} is non-zero is due to ionic fluctuations. These give rise to polarizations in the dielectric media, and surface charge distributions at the interface between the metallic surfaces and the continuum solvent. The potential resulting from the latter can be mimicked by the infinite series of reflected image charges described earlier. First, we note that any given ion (of valency ξ) in the slit will interact with its self-images, i.e. the self-image potential, $V_{self}(z, h)$. This can be obtained from eq. (3) by removing the double sum over ions (i, j), and setting $z_i = z_j \equiv z; \rho_{ij} = 0$:

$$\beta V_{self}(z,h) \approx -\frac{l_b\xi^2}{2}\sum_{k=1,3\ldots}^{k_{max}}\left[\frac{1}{(k-1)h+2z}+\frac{1}{(k+1)h-2z}\right] + \frac{l_b\xi^2}{2}\sum_{m=2,4\ldots}^{m_{max}}\frac{2}{mh} \quad (8)$$

If $k_{max} < m_{max}$, i.e. if n_{max} is an even number, this can be further simplified as:

$$\beta V_{self}(z,h) \approx -\frac{l_B\xi^2}{2}\sum_{l=1}^{l_{max}}\left[\frac{1}{2(h(l-1)+z)}+\frac{1}{2(hl-z)}-\frac{1}{lh}\right] \quad (9)$$

Only including V_{self} will lead to a strong overestimation of the polarization attraction of ions to the surfaces. The reason is because any given ion will be correlated with others, leading to the presence of an atmosphere of opposite charge. The range of the ionic atmosphere will be of order $\sim \kappa^{-1}$, where κ is the inverse Debye-Hückel screening length,

$$\kappa = \left[\sum_i \frac{\beta n_i e^2 \xi_i^2}{\epsilon_r \epsilon_0}\right]^{1/2} \quad (10)$$

Hence, the attractive self-image term for each ion is accompanied by a repulsive contribution, due to the oppositely charged atmosphere. The resulting surface charge distribution at the interface will have cylindrical symmetry (about the z-direction). With this in mind, we propose a simple, yet remarkably accurate, approach to treat image effects. Consider a positive ion at a distance z from a single flat conducting surface, with a dielectric discontinuity at $z = 0$. The mirror charge is then negative, and located at $-z$, with the same x, y coordinates as the original charge. Let us now assume that the opposing image charge from the

ion atmosphere (described above) can be approximated by a circular disc of charge, on the plane at $-z$, centred at the position of the mirror charge. This can be thought of physically as a projection of the cylindrically symmetric ion atmosphere onto the plane containing the self-image charge, which is then approximated as a disc. Thus, an ion in the solution of valency ξ will interact with its self-image (with valency -ξ) and the mirrored atmosphere charge, of valency ξ, uniformly spread out across a circular disc. We shall denote the radius of the disc as R_d; its specific value will be determined by forcing a cancellation of the vdW(0) interaction, as will be described below. The outcomes of this simple approach are:

- The sum {self-image charge + disc charge} is zero, ensuring that the total mirror potential drops to zero when the original charge is far away from the surface
- the potential contribution from {the self-image charge + disc charge} is analytic

A straight-forward integration gives the interaction between a tagged ion at z, and the disc image (at a single surface) as $2\pi l_B[(R_d^2+4z^2)^{1/2}-2z]$. Hence the total image potential, V_{ex}, with two conducting surfaces separated by h, becomes:

$$\begin{aligned}\beta V_{ex}(z,h) \;\approx\; & \beta V_{self}(z,h) \\ & + \frac{l_B\xi^2}{R_d^2}\left(\sum_{k=1,3..}^{k_{max}} \left(R_d^2+((k+1)h-2z)^2\right)^{1/2} + \left(R_d^2+((k-1)h+2z)^2\right)^{1/2} - 2kh\right) \\ & - \frac{2l_B\xi^2}{R_d^2}\left(\sum_{m=2,4...}^{m_{max}} \left(R_d^2+(mh)^2\right)^{1/2} - mh\right) \end{aligned} \tag{11}$$

This potential can then be directly included into the Poisson-Boltzmann approach, to give an *image-corrected* version of the theory, iPB. Thus our theory remains non-linear.

We expect that electrostatic contributions to the surface interactions will be predominately repulsive. As the surfaces are pushed closer together, the salt solution will be pushed out into the bulk. The loss of attractive image interactions leads to an increase of the free energy. This mechanism can be viewed as a type of "ionic desolvation" of the surfaces. This repulsion is counteracted by the vdW(0) attraction, which is not included in the electrostatic free energy. This is because the latter is calculated assuming that the dielectric material responds *passively* to the electrolyte solution. The thermally activated correlation between the metallic surfaces gives rise to the vdW(0) term and must be added separately. The higher-frequency contributions to the van der Waals interaction have a quantum origin and are more specific to the type of material. We will not consider them in this work.

In order to establish the radius, R_d of the counterion disc (see earlier), we invoke an *ansatz* that R_d is proportional to the Debye length κ^{-1}:

$$R_d \propto \frac{1}{\kappa} \tag{12}$$

An important result of our approximate image contribution is that the iPB predicts a long-ranged repulsive electrostatic surface pressure that decays as h^{-3} and which is independent of the salt concentration. This is the same dependence on separation as the vdW(0) contribution. A natural choice for the proportionality constant in Eq.(12) will be that where the electrostatic free energy is exactly cancelled by the vdW(0) interaction at long-range. In other words, writing, $R_d = \alpha\kappa^{-1}$, α is chosen so that the iPB pressure becomes equal to $-P_{vdW}(0)$ at long range. In order to illustrate this process, we show in Figure 1 the asymptotic part of the electrostatic pressure for various choices of α, We find that for monovalent ions in an aqueous solution, at room temperature, the choice:

$$R_d \approx 2.8\kappa^{-1} \tag{13}$$

will cancel the vdW(0) interaction, essentially exactly. An analytic derivation of this value is possible, via asymptotic expansion of the long-range pressure predictions of the iPB,

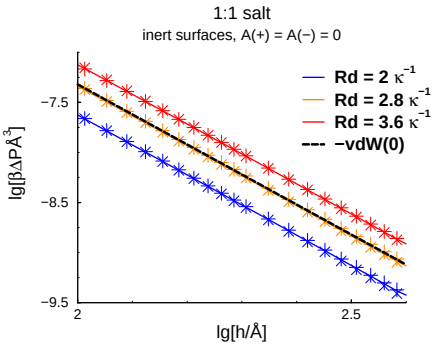

Figure 1: The long-range part of the net pressures, as calculated by iPB. The results for several choices of α, with $R_d = \alpha\kappa^{-1}$, are shown, and the choice $\alpha = 2.8$ leads to an essentially perfect match with $-P_{vdW}(0)$.

however, we will not present that here and content ourselves with a numerical evaluation. When matching the long-ranged tail, it is advantageous to use the interaction free energy, Δg_s, rather than the pressure, as it is a more sensitive quantity (being an integral of the pressure). Examples of this matching are given in Figure 2. The use of the Debye screening

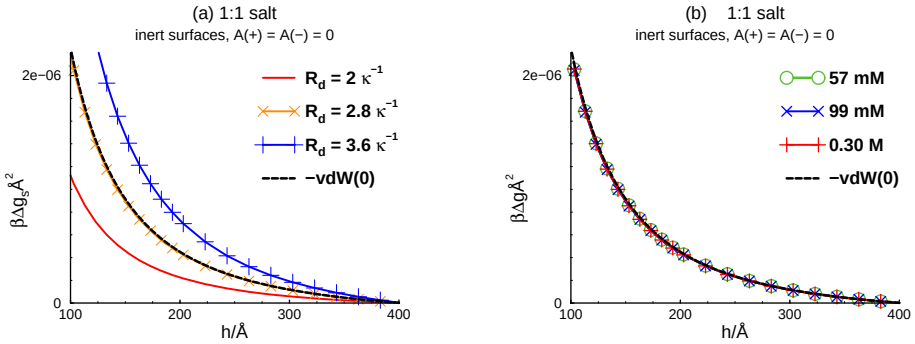

Figure 2: The long-range part of the interaction free energies, as calculated by iPB.
(a) Results with obtained different choices of α (similarly to Figure 1), at 99 mM salt.
(b) Results obtained at various salt concentrations, for the special case of $R_d = 2.8/\kappa$.

length for the characteristic length of the ion atmosphere does *not* imply that we are using a linearized PB theory. This screening length is valid asymptotically and the value of the proportionality constant, α, reflects (among other things) non-linear effects.

It is worthwhile noting here that later in this article will also compare iPB predictions with simulations of dispersions containing 2:1 (or 1:2) salt. For these cases, we will find that the same proportionality constant, α=2.8, will also cancel the vdW(0) contribution. This is because the asymptotic tail of the electrostatic energy is independent of κ. This follows from a fundamental analysis of the electrostatic interaction [16] and, interestingly, is also satisfied by the iPB approximation. One might anticipate that a mean-field theory (such as the iPB) becomes inaccurate for 2:1 salts, however, we shall show that this is not the case. This notwithstanding, the image potential approximation used in the iPB theory can, in principle, be imported to more advanced theoretical treatments, where ion correlation

effects are accounted for.[27–33]

2.4 Ninham-Yaminsky theory (NY)

Ninham and Yaminsky[16] developed an elegant theory of interactions between dielectric surfaces across an electrolyte solution. The theory, which we shall denote as NY, was formulated at the level of a linearized Poisson-Boltzmann approximation. For two perfectly conducting surfaces, their expression for the classical part of the *net* interaction free energy (including the vdW(0) term), can be written as:

$$\beta g_{net}(NY) = \frac{1}{4\pi}\int_0^\infty k \ln[1 - e^{-2sh}]dk \tag{14}$$

where $s = (k^2 + \kappa^2)^{1/2}$. We will partition this free energy into electrostatic and the vdW(0) term as follows,

$$g_{net}(NY) = g_s(NY) + g_{vdW}(0) \tag{15}$$

This allows us to compare directly the electrostatic interactions, that are obtained from simulations and the iPB, with $g_s(NY)$ (or the surface pressure derived from it). Note that the properties of the electrolyte (valency and concentration) only enter the NY expression through the Debye length κ^{-1}.

3 Results

An important convergence (and code) check for both simulations and the iPB theory is that the pressure evaluated either at the surfaces or the mid-plane should agree (see SI). In the case of iPB calculations, the derivative of the grand potential with respect to separation provides a third route to the pressure. However, as we shall see, at very low salt concentrations the simulated wall densities become noisy and the surface evaluation of the pressure is of no practical use. In order to obtain convergence in our simulations, we were forced to use very large systems and a rather high number of reflections in the image potential expression. We have not analyzed the reasons for this in any great detail, but it is presumably related to the fact that the net interactions are composed of large, long-ranged, and counteracting contributions. We have, for instance, found an extremely poor convergence when an odd number of reflections is used (see SI).

Initially, we will investigate inert surfaces, wherein the non-electrostatic ion-surface interactions are either hard or softly repulsive and do not discriminate between the ionic species present. Subsequently, we will also consider cases where an ion adsorption potential acts at the surfaces and is specific to ion type.

3.1 1:1 salt, non-adsorbing surfaces

Here we focus on the simplest case of 1:1 salt, and non-discriminating surfaces. In the first section, we establish the electrostatic (ion-induced) repulsive pressure, and compare it the zero frequency vdW pressure. In the subsequent section we report the result of adding the electrostatic and van der Waals pressure contributions together and integrating to to obtain the"total" interaction free energy (neglecting non-zero frequency van der Waals contributions).

3.1.1 Comparing predictions and simulation data for ion-induced repulsive pressures

In Figure 3, we show the interaction between simple, inert, and hard conducting surfaces, at various salt concentrations. As described earlier, the zero-frequency vdW attraction is

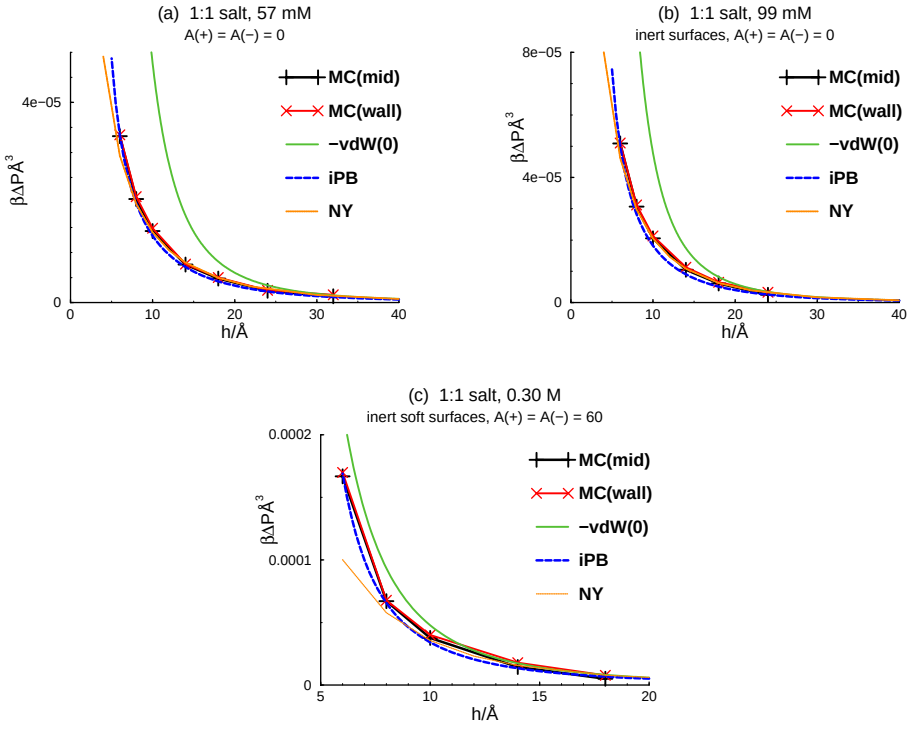

Figure 3: The salt-induced net pressure, ΔP, as obtained by simulation methods (MC), iPB calculations, and NY predictions for the electrostatic component. The negative of the zero frequency vdW pressure ($-P_{vdW}(0)$) is also shown for comparison. The conducting surfaces are non-discriminating ($A_+ = A_-$). At the highest salt concentration, statistical noise was reduced (for the wall pressure) by the use of softly repulsive surfaces.
(a) 57 mM, hard surfaces
(b) 99 mM, hard surfaces
(c) 300 mM, softly repulsive surfaces.

not accounted for in the electrostatic interaction free energy. Instead we show $-P_{vdW}(0)$ separately with its sign reversed. We see that this term dominates the repulsive electrostatic interaction, i.e., this system will overall display a net attractive interaction, even without the additional higher frequency (quantum) contributions to the vdW attraction. The predictions of the iPB and NY theories for the electrostatic interaction are in very good agreement with the simulations.

Note that the repulsive electrostatic pressure *increases* with added salt, approaching $-P_{vdW}(0)$ from below, even at short range. This behaviour is opposite to standard DLVO predictions between charged non-conducting particles, where the electrostatic repulsion *drops* when more salt is added. The *total* net pressure, obtained by adding $P_{vdW}(0)$ to the electrostatic contribution will thus show a diminished range upon the addition of salt. This amounts to a *reduction of a net attractive pressure*. In other words, adding salt to this system would tend to stabilize the dispersion, or at least make it less unstable (with, presumably, slower flocculation rates). This is consistent with the NY prediction, that the total interaction between surfaces in the presence of electrolyte can be described as a screened zero-frequency vdW force.[16,21] In fact, at the highest investigated concentration ($300mM$), the salt-induced repulsion is strong enough to almost completely offset the attractive contribution from $P_{vdW}(0)$, even at short-range. As an aside, we note that this finding would be

relevant to the stability of conducting nanoparticle dispersions in room temperature ionic liquids, where the salt concentration is extremely high.

Comparisons between the pressures evaluated across the mid-plane and at the surfaces, show agreement whenever statistics admits this comparison. These checks are reported and discussed in the SI. At high salt, we encountered a substantial increase in the noise, primarily related to a reduced number of sampled configurations per ion, which was particularly problematic for pressures evaluated at surface contact (these require numerical extrapolations). In order to circumvent this problem, we utilized soft repulsive walls, for the highest investigated salt concentration (300 mM). In the SI, we illustrate that the pressures obtained for hard and softly repulsive ($A_+ = A_- = 60$) walls were nearly identical, except at very short separations.

3.1.2 Net interaction free energies, including vdW(0)

In Figure 4, we demonstrate the agreement between iPB and NY predictions for 1:1 salts, by plotting the net interaction free energy at 57 mM, where the vdW(0) contribution has been included, in order to obtain the complete (classical) interaction between the surfaces. The comparison clearly demonstrates that the two approaches provide nearly identical pre-

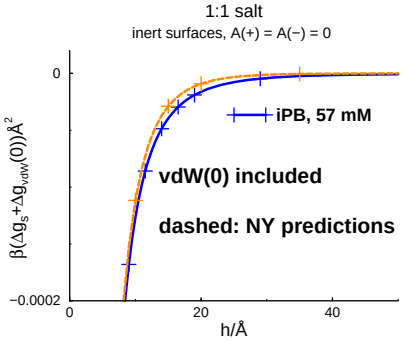

Figure 4: iPB and NY predictions of net interaction free energies in a 1:1 salt solution, as obtained by adding the salt induced (Δg_s) and zero frequency vdW ($\Delta g_{vdW}(0)$) contributions, at various salt concentrations (in the NY theory, both of these terms are included in eq. (14).) The surfaces are hard, non-discriminating ($A_+ = A_- = 0$), and conducting.

dictions in this case.

3.2 2:1 salts, non-adsorbing surfaces

We now turn our attention to asymmetric salts, specifically 2:1 (or 1:2) salts. Here we shall study three important aspects:

- verify that the choice $\alpha = 2.8$ in the iPB interaction will again negate the zero frequency van der Waals pressure
- compare iPB and NY predictions for the electrostatic component of the pressure with simulations
- compare the iPB and NY predictions for the net total interaction free energy, i.e., after adding the zero order van der Waals component.

3.2.1 Verifying that $\alpha = 2.8$

As for 1:1 salts, we will use the criterion that the long-ranged tail of the electrostatic component of the free energy will match $-g_{vdW}(0)$ in order to determine the radius, R_d of the image disc in the iPB approximation. As shown in Figure 5, the choice $R_d \approx 2.8\kappa^{-1}$, i.e., the same value for α as was used in the 1:1 salt will accomplish this cancellation. There is a deeper reason for this, as the asymptotic form of the iPB is independent of the Debye length. We shall demonstrate this and an analytic derivation for the value of α in a subsequent publication.

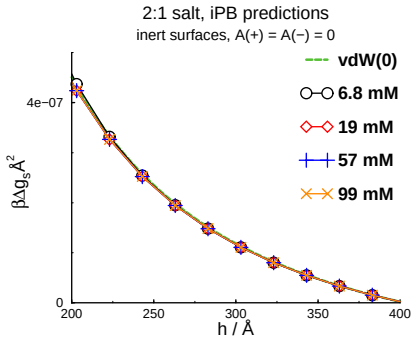

Figure 5: iPB predictions for the long-range part of the interactions between non-discriminating ($A_+ = A_- = 0$) and conducting surfaces immersed in a 2:1 solution. Eq. (13) was used, for each salt concentration, to establish the value of R_d (common to both ions).

3.2.2 Comparisons with simulation data for ion-induced repulsive pressures

In Figure 6, we show the electrostatic interactions between hard conducting surfaces, at various salt concentrations. Here the inaccuracy of the NY theory becomes apparent. As a linearized mean-field theory for electrolytes, it depends purely on the Debye length κ^{-1} and does not differentiate between solutions containing salts of different valency, if they have the same ionic strength. Furthermore, the NY theory will always predict that the total interaction is a screened van der Waals interaction, ie., will always be attractive. However, the simulation data clearly shows that the electrostatic repulsion for 2:1 salts more than compensates for the zero frequency vdW attraction, i.e., the approach towards -vdW(0) at long range, occurs *from above*. This result is faithfully captured by the iPB theory and, remarkably, the accuracy of iPB appears to be slightly better relative to the case of 1:1 salts. This is probably due to a cancellation effect. As in any mean-field theory, the iPB neglects ion correlations. Correlations will tend to increase the adsorption of ions at the conducting surface, relative to a mean-field prediction, as they allow the ions to pack more densely at the surface. This increased adsorption will tend to generate a more repulsive electrostatic pressure, but this is counteracted by the fact that lateral ion correlations across the mid-plane will lead to a more attractive pressure than would be predicted by a mean-field theory.

3.2.3 Net interaction free energies, including vdW(0)

The resulting iPB and NY predictions for the total net interaction free energies, i.e. the sum of the repulsive ion pressure and the attractive vdW(0), are shown in Figure 7. The

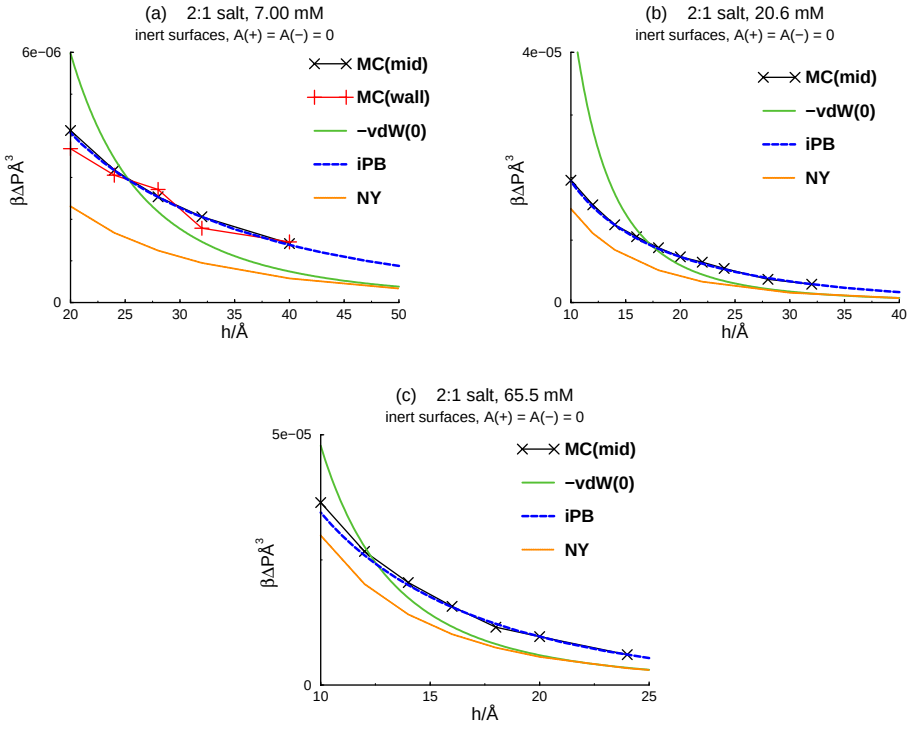

Figure 6: The salt-induced net pressure, ΔP, as obtained by simulation methods (MC), and iPB or NY calculations, respectively. The negative values of the zero frequency vdW attraction are also shown, as reference (-vdW(0)). The walls are conducting, but non-discriminating. Due to the significant noise, the wall pressure is only displayed for the lowest salt concentration.
(a) 7.00 mM
(b) 20.6 mM
(c) 65.5 mM

demonstrated accuracy of the iPB suggests that its predictions may be regarded as somewhat of a benchmark, especially in those systems where simulations prove to be statistically unreliable. Our results also clearly show that the NY approach leads to qualitatively incorrect results for multivalent ions. The results for this system may be of some relevance to the stability of gold sols in solutions of organic acid. For example, we have seen how a free energy barrier may eventuate (in the absence of steric stabilizers) when multivalent ions are present. It is possible that this stability may be enhanced due to adsorption of multivalent citric(or ascorbic) acid ions onto the gold particles. At pH 7 citric acid is primarily trivalent in a bulk solution.

3.3 1:1 salt, ion-specific adsorption

In this section, we shall analyze the effect of introducing an ion-specific adsorption potential at the surfaces, in a 1:1 salt solution. As already mentioned, it is generally believed that adsorption is important for the stability of metal particles of colloidal size. We model the surface specificity by setting $A(+) = 4.5$ and $A(-) = -4.5$, i.e., we assume that the anions are adsorbed more strongly than cations. A possible mechanism leading to this discrimination is due to ion hydration, whereby the cations (typically being strongly hydrated by

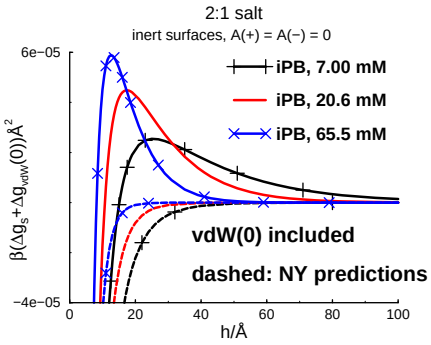

Figure 7: iPB predictions of total interaction free energies, as obtained by adding 2:1 salt induced (Δg_s) repulsions and zero frequency vdW ($\Delta g_{vdW}(0)$) attractions, at various salt concentrations. The surfaces are non-discriminating ($A_+ = A_- = 0$) and conducting.

water) are effectively repelled from the surfaces.

3.3.1 Comparing predictions and simulation data for ion-induced repulsive pressures

Figure 8 shows the repulsive electrostatic pressure at various salt concentrations in the presence of the discriminating surfaces described above. To the best of our knowledge, the NY theory has not been generalized to account for ion adsorption, so no predictions from that theory are presented here.

In Figure 8(a) (at 6.8 mM salt), we see that the iPB proves to be reasonably accurate, only slightly underestimating the repulsion. We note, however, that these forces are measured at relatively long range, where the pressures are weak, and the observed differences may also be due to uncertainty in our estimate of the bulk pressure in the simulations. At this low salt concentration simulated pressures, evaluated at the surfaces, were noisy on this scale and are not given. The reason is the dramatically varying density profiles, primarily the anions, in the vicinity of the walls. This makes accurate extrapolations of the density profiles difficult leading to large relative uncertainties when the net pressures as weak as they are at these large distances. One interesting observation is that ion specific adsorption generates a strong repulsion that exceeds $-P_{vdW}(0)$ at long range. We note, however, the latter dominates at short separations, which results in a non-monotonic total interaction.

In Figure 8 (b), at about 19 mM, this behaviour is even more apparent whereby the total interaction is clearly repulsive at long range, but turns attractive at short separations. This is the same qualitative behaviour as predicted by the standard DLVO model for charged particles without dielectric discontinuities, though we note that the particles considered here are uncharged. The iPB approximation again proves to be very accurate, which is an encouraging observation as the simulations are computationally expensive. On the other hand, the iPB calculations are quickly obtained at high precision. The results at a salt concentration of 57 mM are presented in Figure 8 (c). The simulated pressures include those evaluated at the surface (as well as across the midplane) as the bulk concentration is now high enough to allow density extrapolations with a relatively high precision. The substantial increase in repulsion at large surface separation, brought about by ion specific adsorption, can be appreciated by comparing with the results obtained for non-adsorbing surfaces, cf. Figure 3. We again note there is almost quantitative agreement between the simulations and the iPB predictions.

At even higher salt concentrations, Figure 8 (d), the electrostatic repulsion dominates

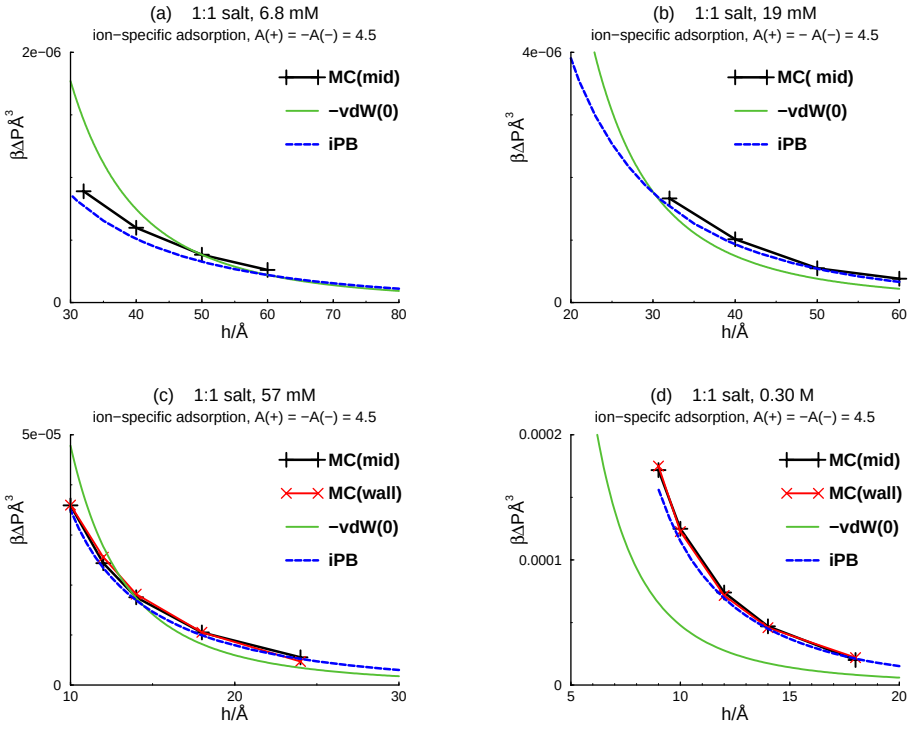

Figure 8: Interactions between ion-discriminating ($A_+ = -A_- = 4.5$) and conducting surfaces, immersed in salt solutions. The notation is the same as in Figure **??**.
(a) 6.8 mM salt
(b) 19 mM salt
(c) 57 mM salt
(d) 0.30 M salt

$P_{vdW}(0)$ for all simulated separations. The two will of course merge at long range, but the total interaction will approach zero from *above*. These results suggest that ion-specific adsorption may *completely* stabilize dispersions of conducting particles at high salt concentration. [1]. This prediction will naturally depend upon the strength of the finite frequency van der Waals pressure, which is not considered here. Nevertheless, from a fundamental point of view, this is an interesting observation and one which would be substantially amplified in an ionic liquid. The long-ranged tail of the interaction free energy is investigated in the SI, where we confirm that the electrostatic component, obtained by the iPB theory, cancels the zero frequency van der Waals term.

3.3.2 Net interaction free energies, including vdW(0)

A summarizing graph of the *total* interaction free energies, for systems with ion-specific adsorption, is given in Figure 9. We see how an increased salt concentration sees a gradual build-up of the repulsive regime. At intermediate concentrations, this leads to a free energy barrier, but at high concentrations, the interaction free energy is repulsive at all separations.

[1] Adding a non-adsorbing salt will of course not have the same effect.

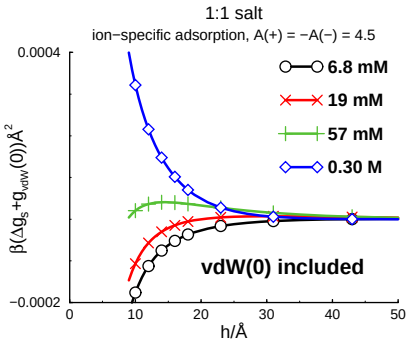

Figure 9: iPB predictions of total interaction free energies, as obtained by adding the salt induced (Δg_s) and zero frequency vdW ($\Delta g_{vdW}(0)$) contributions, at various salt concentrations. The surfaces are ion-discriminating ($A_+ = -A_- = 4.5$) and conducting.

3.3.3 Comparing with charged surfaces without images

The stability of dispersions containing metal nanoparticles is often attributed to ion-specific adsorption, effectively charging up the particles. The results presented above support this suggestion. On the other hand, DLVO treatments generally neglect effects from image interactions and only include a combination of double layer repulsions and van der Waals attractions. It is instructive to try to map our model to the simpler one envisaged in DLVO calculations on charged surfaces.

We consider the 19 mM system, with ion-specific adsorption, as illustrated in Figure 8 (b). The adsorption potential gives an excess of anions close to the surface, which can be interpreted as producing a surface-bound charge density. It is useful to define an effective z-dependent, surface charge density, $\sigma(z)$, as:

$$\sigma(z) = \int_0^z n_+(z') - n_-(z')dz' \tag{16}$$

The quantity is plotted for our system in Figure 10 (a). A "natural" choice for the effective surface-bound charge density is the minimum value of $\sigma(z)$. In this case, we obtain from Figure 10 (a) $\sigma_{eff} \approx -0.0001e/\text{Å}^2$. This value remains relatively insensitive to the distance between the surfaces. We now construct a standard double-layer model, with two charged surfaces, separated by a salt solution. The charge density on the surfaces are set to σ_{eff}. As in the usual DLVO approach, we perform PB calculations *neglecting the effect of the dielectric discontinuities*. The density profiles against a single surface are illustrated in Figure 10(b). We see that, beyond about 25 Å from the surface, the ion density profiles of the simple double-layer model agree quite well with those obtained with the iPB. The total surface interactions are displayed in Figure 10(c). The agreement is reasonable at long range, but deteriorates for separations below $h = 80$Å or sos. The surfaces with adsorbing ions shows a maximum at $h \approx 80$Å, below which the vdW term dominates. On the other hand the system at constant surface charge predicts a repulsion in this region. To summarize, the long-ranged behaviour can probably be modelled using a fixed effective surface charge and no image effects, but substantial errors can be expected at short range.

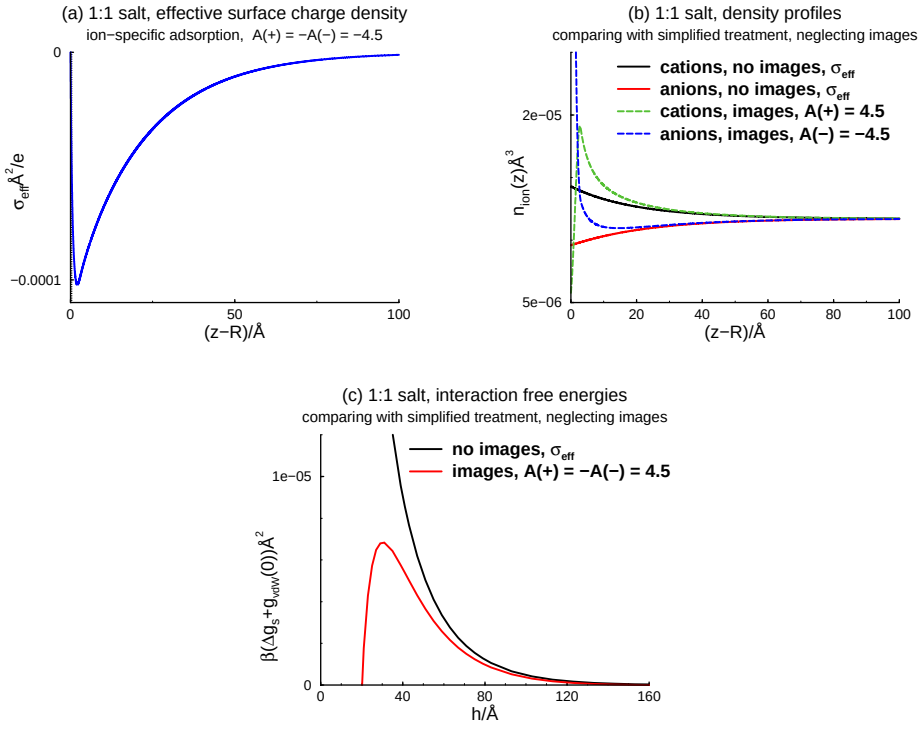

Figure 10: Comparing interactions and density profiles between ion-discriminating ($A(+) = -A(-) = 4.5$) conducting surfaces, and a simple "analogue", with non-conducting surfaces (see main text. The salt concentration is 19 mM
(a) Effective surface charge density at the conducting surface.
(b) Corresponding ion density profiles, at the conducting and the "simplified" (see text) surfaces, respectively.
(c) Corresponding interaction free energies.

4 Conclusions and outlook

We have studied the interaction of conducting particles immersed in electrolyte solutions. Computer simulations for non-adsorbing neutral surfaces show that the electrostatic contribution, to the surface interactions is repulsive, due to an ionic solvation effect. That is, the ions in solution are attracted to the surfaces via polarization (modelled by image charges) and as the surfaces approach, ions are excluded from the interstitial region of favourable interactions. On the other hand, the electrostatic contribution does not contain the vdW contribution to the free energy. The zero-frequency contribution of the latter exactly cancels the long-ranged repulsion of the electrostatic interaction. When added to the electrostatic interaction, we find that the force between the surfaces becomes attractive, albeit, screened by the salt. Indeed, the attraction diminishes as the salt concentration increases. The Ninham-Yaminsky (NY) theory is very accurate for 1:1 salt solutions against non-adsorbing surfaces. As far as we know, this is the first time that the accuracy of this theory has been evaluated against simulations. However, the NY approach generates qualitatively incorrect net interactions for solutions containing asymmetric (M:1 or 1:M) salts. Furthermore, we are not aware of the generalization of the NY theory to adsorbing surfaces. Our simulations show that if the surfaces are able to specifically adsorb ions they obtain a residual net charge, and the interaction becomes more repulsive. We find that even with the addition

of the zero-frequency vdW contribution, such surfaces may be completely repulsive at high enough salt concentration.

In addition to the simulations, we have proposed a simple correction to the Poisson-Boltzmann theory, the so-called image Poisson-Boltzmann, which accounts for the dielectric discontinuity. The resulting theory is surprisingly accurate, even for an asymmetric 2:1 (or 1:2) salt, giving essentially quantitative agreement with the simulations, even when the NY theory is qualitatively incorrect. For instance, the total surface interactions in 2:1 (or 1:2) salt solutions are *repulsive* at long range. This is nicely captured by iPB, whereas NY theory predicts a monotonic attraction. The iPB theory may prove a useful adjunct to studies on systems with dielectric inhomogeneities, especially as simulations of these systems are numerically demanding. An important additional advantage of the iPB approach is that ion-specific adsorption can be included in the theory without loss of accuracy. The ability to account for ion-specificity is of crucial importance for studies on metal particle dispersions, such as gold sols. For instance, it has been been hypothesized that trivalent citric acid anions are displaced by monovalent gold tetrachloride anions, at the surface of gold particles. This study clearly shows that such displacements will require a very strong preferential adsorption of the monovalent species. Finally, given the density functional formulation of the iPB it would be relatively straightforward to move beyond the mean-field level, and to include other mechanisms, such as excluded volume effects. Additionally, realistic models of oligomeric ions, as for example, occur in room temperature ionic liquids is also possible.

5 Acknowledgment

J.F. acknowledges financial support by the Swedish Research Council.

References

[1] M. Faraday, *Philosophical Transactions of the Royal Society of London*, 1857, **147**, 145–181.

[2] J. Turkevich, P. C. Stevenson and J. Hillier, *Discuss. Faraday Soc.*, 1951, **11**, 55–75.

[3] M.-C. Daniel and D. Astruc, *Chemical Reviews*, 2004, **104**, 293–346.

[4] D. Goia and E. Matijevi, *Colloids and Surfaces A: Physicochemical and Engineering Aspects*, 1999, **146**, 139 – 152.

[5] D. Andreescu, T. K. Sau and D. V. Goia, *Journal of Colloid and Interface Science*, 2006, **298**, 742 – 751.

[6] V. Amendola and M. Meneghetti, *Phys. Chem. Chem. Phys.*, 2009, **11**, 3805–3821.

[7] M. A. Uppal, A. Kafizas, T. H. Lim and I. P. Parkin, *New J. Chem.*, 2010, **34**, 1401–1407.

[8] C. Li, D. Li, G. Wan, J. Xu and W. Hou, *Nanoscale Research Letters*, 2011, **6**, 440.

[9] V. Merk, C. Rehbock, F. Becker, U. Hagemann, H. Nienhaus and S. Barcikowski, *Langmuir*, 2014, **30**, 4213–4222.

[10] C. H. Munro, W. E. Smith, M. Garner, J. Clarkson and P. C. White, *Langmuir*, 1995, **11**, 3712–3720.

[11] B. V. Derjaguin and L. Landau, *Acta Phys. Chim. URSS*, 1941, **14**, 633–662.

[12] E. J. W. Verwey and J. T. G. Overbeek, *Theory of the Stability of Lyophobic Colloids*, Elsevier Publishing Company Inc., Amsterdam, 1948.

[13] S. Biggs, M. Chow, C. F. Zukoski and F. Grieser, *Journal of Colloid and Interface Science*, 1993, **160**, 511 – 513.

[14] S. Biggs and P. Mulvaney, *The Journal of Chemical Physics*, 1994, **100**, 8501–8505.

[15] R. Kjellander and S. Marcelja, *Chemical Physics Letters*, 1987, **142**, 485 – 491.

[16] B. W. Ninham and V. Yaminsky, *Langmuir*, 1997, **13**, 2097–2108.

[17] M. Boström, D. Williams and B. Ninham, *Phys. Rev. Lett.*, 2001, **87**, 168103.

[18] M. Boström, D. R. M. Williams and B. W. Ninham, *Langmuir*, 2002, **18**, 8609–8615.

[19] B. Jancovici and L. Samaj, *Journal of Statistical Mechanics: Theory and Experiment*, 2005, **2005**, P05004.

[20] P. Buenzli, *Ph.D. thesis*, Ecole Polytechnique, Lausanne, 2006.

[21] M. Boström, V. Deniz, G. Franks and B. Ninham, *Advances in Colloid and Interface Science*, 2006, **123126**, 5 – 15.

[22] M. M. Hatlo and L. Lue, *Soft Matter*, 2008, **4**, 1582–1596.

[23] M. Kanduc, A. Naji, J. Forsman and R. Podgornik, *The Journal of Chemical Physics*, 2012, **137**, 174704.

[24] B. V. Derjaguin, *Kolloid Zeits.*, 1934, **69**, 155.

[25] J. Mahanty and B. Ninham, *Dispersion forces*, Academic Press, 1976.

[26] G. M. Torrie and J. P. Valleau, *J. Chem. Phys.*, 1980, **73**, 5807–5816.

[27] S. Nordholm, *Aust. J. Chem.*, 1984, **37**, 1.

[28] J. Forsman, *J. Phys. Chem. B*, 2004, **108**, 9236.

[29] C. W. Outhwaite and L. B. Bhuiyan, *J. Chem. Soc., Faraday Trans. 2*, 1983, **79**, 707.

[30] L. Guldbrand, B. Jönsson, H. Wennerström and P. Linse, *J. Chem. Phys.*, 1984, **80**, 2221.

[31] R. Kjellander, *J. Chem Soc. Faraday Trans. 2*, 1984, **80**, 1323.

[32] L. Mier-y Teran, S. Suh, H. S. White and H. T. Davis, *J. Chem. Phys.*, 1990, **92**, 5087.

[33] J. Forsman, *J. Chem. Phys.*, 2009, **130**, 064901.